

Response functions of spiral waves in the FitzHugh-Nagumo system

Grigory Bordyugov*

*Institut für Physik und Astronomy, Universität Potsdam,
Karl-Liebknecht-Strasse 24/25 14476 Potsdam-Golm Germany*

(Dated: November 1, 2008)

Spiral waves are rotating solutions of nonlinear reaction-diffusion systems in two spatial dimensions. Due to the symmetries of the plane, a spiral wave can be shifted and rotated arbitrarily, still remaining a solution to reaction-diffusion system. Introducing a symmetry-breaking perturbation of the reaction-diffusion equation, the spiral wave begins to drift, i.e. change its rotation phase and its position on the plane. On the linear level (for small perturbations), the velocity of drift can be calculated using the perturbation technique, projecting on the symmetry subspaces of the unperturbed equation. For the projection one needs the eigenfunctions of the adjoint problem, since the linearization of reaction-diffusion problem is not self-adjoint. Those adjoint eigenfunctions are called response functions of spiral waves. In this paper, I will present results of computations of response functions and compare the predictions of drift velocities with the help of those with the direct numerical simulations of drifting spirals in reaction-diffusion system. Both results turn out to be in a nearly perfect quantitative agreement.

PACS numbers: Valid PACS appear here

Keywords: Spiral waves, response functions, drift of spiral waves

I. INTRODUCTION

Spiral waves are probably the most beautiful example of spatio-temporal pattern formation in active media. They have been experimentally observed in a variety of physical, chemical and biological systems [1–4] as well as in simple model equations, which are usually of the reaction-diffusion type. The most important motivation to study spirals comes from the observations that in the human heart, emergence of spiral waves can lead to arrhythmias, i.e. incoherent cardiac muscle contraction [2, 5], which often can lead to death.

Spiral waves are known to drift when subjected to a (resonant periodic) forcing [6–8] as well as in medium inhomogeneities [9]. The idea to describe slow drift of spiral waves with the help of response functions originates from [10]. In that paper, projecting the linearized perturbed equation on the Goldstone eigenmodes of the unperturbed problem resulted in three simple equations for the position and the relative phase of the perturbed spiral. The strong localization of response functions assures that only perturbations near the core affect the dynamics of the spiral wave. For an experimentalist, the localized sensitivity of spiral waves is a common and natural observation [6]. On the rigorous mathematical level, the localization of response functions follows from the Fredholm properties of the linearization about the spiral [11]. A group-theoretical approach to describe drift of spirals was formulated in [12–15].

Let me review some previous results on response functions. A huge body of results on response functions of spiral waves in the complex Ginzburg-Landau equation

(CGLE) [16–20] is available. There, drift velocities of spirals in the CGLE were also computed with the help of response functions. Due to the structure of the CGLE, the existence, stability and the adjoint problems are merely ODEs in polar radius and hence can easily be cracked by boundary problem solvers. For the FitzHugh-Nagumo model [21], there have been calculations of response functions, based on time integration of the linear adjoint problem, however, no drift velocities were calculated.

This paper describes results of calculation of response functions for rigidly rotating spiral waves in the FitzHugh-Nagumo equations. I follow the ideas by Barkley to compute the spiral waves as an equilibrium in the rotating frame by a number of Newton iterations and then to compute some of the eigenvalues of the linearized problem using indirect iterative methods, see [22, 23]. I also compute drift velocities predicted by the response functions and compare them to the results of direct time integration of the perturbed reaction-diffusion system.

II. SETUP AND MAIN ASSUMPTIONS

I consider the following reaction-diffusion system on the whole plane \mathbb{R}^2 :

$$\partial_t u = f(u) + D\Delta u + \epsilon h, \quad (1)$$

where $u = u(r, \theta, t) \in \mathbb{R}^\ell$ is an ℓ -valued vector of species, $f(u)$ is a sufficiently smooth reaction kinetics, Δ is the 2D Laplace operator, modeling the diffusion of species, and h is a generic bounded perturbation with a small strength ϵ . Here, $(r, \theta, t) \in \mathbb{R}^+ \times [0, 2\pi) \times \mathbb{R}$ denote the laboratory polar coordinates and time. Matrix D denotes the $\ell \times \ell$ diffusion matrix with non-negative entries.

*Electronic address: Grigory.Bordyugov@uni-potsdam.de

A. Unperturbed spirals

I assume that for $\epsilon = 0$, Eq. (1) supports a rigidly rotating spiral wave in the form of

$$u(r, \theta, t) = q(r, \theta - \omega t)$$

with the rotation frequency ω . The spiral wave solution q hence solves the nonlinear existence equation for spiral waves in the rotating frame of reference $(r, \theta, t) \rightarrow (r, \theta - \omega t, t)$:

$$D\Delta q + \omega \partial_\theta q + f(q) = 0. \quad (2)$$

For an experimentalist, it is always possible to place a video camera in front of the spiral in such a way and to rotate it with an appropriate angular frequency that the spiral would appear steady on the recorded footage. For the spiral q , one can define its tip as the point on the plane with prescribed value of q . For rigidly rotating spirals, the tip trajectory is always a circle, see Fig. 1 (b).

Given the spiral q as a solution of the nonlinear existence problem Eq. (2), one can raise the question of the stability of the spiral. On the linear level, the stability is determined by the eigenvalue problem

$$\begin{aligned} \mathcal{L}v &= \lambda v, \\ \mathcal{L} &:= f_u(q) + \omega \partial_\theta + D\Delta, \end{aligned} \quad (3)$$

where $\lambda \in \mathbb{C}$ is an eigenvalue and $v : \mathbb{R}^2 \rightarrow \mathbb{C}^\ell$ is the corresponding eigenfunction. Spiral q is unstable if there are some eigenvalues λ of the stability operator \mathcal{L} with positive real part, otherwise spiral is stable. In the following, I assume that spiral q is stable and \mathcal{L} has no spectrum in the open complex right half-plane.

The symmetry with respect to shifts and rotations is reflected in the spectrum of the linearization \mathcal{L} about the spiral. When considered on the whole plane \mathbb{R}^2 , the operator \mathcal{L} has three critical eigenvalues on the imaginary axis, given by

$$\begin{aligned} \lambda_0 &= 0, \\ \lambda_{\pm 1} &= \pm i\omega. \end{aligned}$$

The zero eigenvalue reflects the rotation symmetry, and the corresponding eigenfunction is given by $v_0 = \partial_\theta q$ (differentiate Eq. (2) with respect to θ). Indeed, an infinitesimal rotation is merely a shift in θ by a small angle $\delta\theta$, and we have $q(r, \theta - \omega t - \delta\theta) \approx q(r, \theta - \omega t) - \delta\theta \partial_\theta q(r, \theta)$. Thus, a small rotation is equivalent to subtracting $\partial_\theta q(r, \theta)$ weighted by the amount of rotation.

The pair of complex conjugate $\lambda_{\pm 1}$ have as eigenfunctions $\partial_x q \pm i\partial_y q$, where x and y are the Cartesian coordinates with the origin at the centre of rotation of q . These eigenvalues reflect the translational symmetry of the spiral. Analogously to rotation, any infinitesimal translation can be represented as an addition of a linear combination of $v_{\pm 1}$ to the original spiral $q(r, \theta)$.

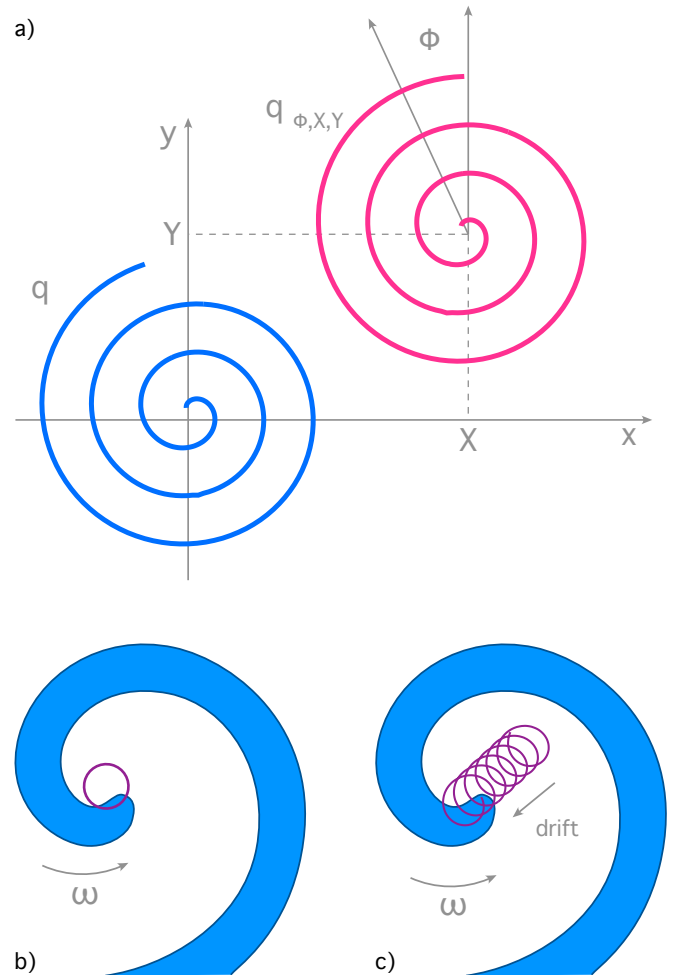


FIG. 1: a) Blue curve denotes the reference spiral q whose centre of rotation is located at the coordinate origin. Red curve denotes another spiral $q_{\Phi, X, Y}$, which is rotated by Φ and shifted by $(X, Y)^+$ in comparison to the reference spiral. b) Tip of rigidly rotating spiral draws a circle. Arrowed arc shows the direction of spiral rotation. c) Tip of drifting spiral draws a cycloid. Arrowed arc shows the direction of spiral rotation and arrowed straight line shows the direction of spiral drift. Drift may also occur along a non-straight trajectory.

In the following I will also need \mathcal{L}^+ , the adjoint to \mathcal{L} [27]. Note that both on the whole plane \mathbb{R}^2 and on bounded disks with either Neumann or Dirichlet boundaries with the standard scalar product, the adjoint \mathcal{L}^+ is given by:

$$\mathcal{L}^+ = f_u^+(q) - \omega \partial_\theta + D\Delta.$$

The adjoint \mathcal{L}^+ also has three eigenvalues $\mu_{0, \mp 1}$ with the corresponding eigenfunctions $w_{0, \mp 1}$. The eigenfunctions of \mathcal{L} and those of the adjoint \mathcal{L}^+ satisfy the biorthogonality condition:

$$\langle w_i, v_j \rangle = \delta_{ij}, \quad i, j = 0, \pm 1.$$

The Euclidean symmetry of the problem lifts the spiral

$q(r, \theta - \omega t)$ to a family of spirals, parameterized by the relative phase shift Φ and the coordinate shift $(X, Y)^+$ with respect to the reference spiral q , please compare Fig. 1 (a). Throughout the paper I will formally denote a spiral which is rotated by Φ and shifted by $(X, Y)^+$ with respect to the reference spiral by

$$q_{\Phi, X, Y}.$$

Strictly speaking, the symmetries do not persist when truncating to a finite domain, which is more physically relevant [24]. The rotational and translational eigenvalues of the spiral may shift off the imaginary axis. However, spirals do not particularly care about the existence of domain boundaries as long as the spirals are sufficiently far from boundaries. This experimentally obvious phenomenon will become more clear in the following section, where I'll describe the localized sensitivity of spirals.

B. Drift equations

Introducing $\epsilon \neq 0$ in Eq. (1) can break the symmetry of Eq. (1) and make spirals *drift*. The centre of rotation $(X, Y)^+$ of a drifting spiral and its relative phase Φ slowly depend on time. The tip of the drifting spiral draws a cycloid, see Fig. 1 (c).

Let me mention two most important examples of the symmetry breaking perturbations h which have been often considered in the literature:

1. Resonant drift: In this case, the perturbation h is a periodic function of time only: $h = h(t) = h(t + L)$ and its L period equal or close to the rotation period of the spiral $\frac{2\pi}{\omega}$.
2. Drift in inhomogeneities: The perturbation h depends on space $h = h(r, \theta)$ and represents a variation of medium parameters in space. The simplest case is a constant-gradient perturbation such that $\nabla h = \text{const}$.

Further examples include drift due to interactions with domain boundaries, drift due to interaction between two spirals, etc.

Biktaşev *et al.* [10] suggested that for perturbed Eq. (1) the following ansatz can be used:

$$u = q_{\Phi(\epsilon t), X(\epsilon t), Y(\epsilon t)} + \epsilon s. \quad (4)$$

This is nothing else but a spiral which drifts at an ϵ -slow rate plus some ϵ -small correction s which accounts for a possible deformation of the spiral form. After substitution of the Ansatz 4 in Eq. (1) and projection with the help of the adjoint eigenfunctions $w_{0, \pm 1}$, one obtain the following drift equations:

$$\begin{aligned} \dot{\Phi} &= -\epsilon \langle w_0, h \rangle, \\ \dot{X} &= -2\epsilon \text{Re} \left[e^{-i(\omega t + \Phi)} \langle w_1, h \rangle \right], \\ \dot{Y} &= 2\epsilon \text{Im} \left[e^{-i(\omega t + \Phi)} \langle w_1, h \rangle \right]. \end{aligned} \quad (5)$$

Substituting the spatial delta function instead of the perturbation h in Eq. (5), we see that $w_{0, \pm 1}$ tell us how sensitive the spiral is at the given location. That's why Biktaşev and co-authors decided to pick up the term *response functions* to name the adjoint eigenfunctions $w_{0, \pm 1}$, thus providing us with a nice intuitive description of quite abstract mathematical objects like eigenfunctions of adjoint operator.

Eqs. (5) also suggest that the adjoint eigenfunctions $w_{0, \pm 1}$ are localized in space. Indeed, consider the resonant drift of spirals on the whole plane. In this case, h is not localized, since it doesn't depend on the space at all. The drift velocity however must be finite, thus suggesting that the scalar products in Eq. (5) must converge even for infinitely large domain size.

Usually, the magnitude of the drift velocity is more interesting than its direction. For time-periodic perturbations of period $L = \frac{2\pi}{\Omega}$ (where Ω is the frequency of the perturbation), one can average Eq. (5) over L , obtaining

$$\begin{aligned} \dot{\Phi} &= \omega - \Omega - \epsilon H_0, \\ \dot{X} &= 2\epsilon |H_1| \cos \varphi, \\ \dot{Y} &= 2\epsilon |H_1| \sin \varphi, \end{aligned} \quad (6)$$

where H_n is the n -th Fourier component of the projection of the perturbation h on w_n :

$$H_n = \frac{1}{L} \int_{t-L/2}^{t+L/2} dt e^{-in\Omega t} \langle w_n, h(t) \rangle,$$

where we omitted the spatial dependence of perturbation h for the sake of brevity. In the equations above, φ is the difference between the phase of the spiral and the phase of the external perturbation: $\varphi = (\omega - \Omega)t + \bar{\Phi} + \arg H_1$, the bar represents an average over the time period L .

Note that both resonant drift and drift in gradients represent examples of periodic perturbations. The former is obvious, whereas in the latter one should keep in mind that the adjoint eigenfunctions $w_{0, \pm 1}$ are functions of the rotating angle $\theta - \omega t$ and the gradient which is time-independent in the laboratory coordinate is time-periodic in the rotating coordinate frame.

III. METHODS

The challenge of computing response functions for rigidly rotating spiral waves consists of two sub-tasks: First, one has to solve the nonlinear problem Eq. (2) in order to compute spiral $q(r, \theta - \omega t)$ itself, and secondly one has to compute three critical eigenvalues of the matrix, which represents the discretized stability operator \mathcal{L} and its adjoint \mathcal{L}^+ .

Numerically, both tasks were solved on a disk domain of radius R with Neumann boundary conditions. I used a polar grid with N_θ equidistant angular discretization

points and N_r radial equidistant discretization points plus one point in the origin. This scheme thus produced a set of $N = \ell(1 + N_r N_\theta)$ real values to approximate the spiral and N complex values to approximate a complex-valued eigenfunction of the linearization or adjoint. The Laplace operator was formulated in the polar coordinates. I used a pseudospectral approximation for angle derivatives and three-point scheme for radial derivative. In the origin, the Laplace operator was computed as an average over $N_\theta/4$ five-point stencils.

a. Nonlinear problem Back in 1992, Barkley [22] successfully used the Newton method in order to solve the nonlinear problem and to compute spiral waves and I stick to the same method. Since the Newton method involves solving a larger system of linear equations for the Jacobian matrix of the nonlinear problem, one has to choose such representation of the solutions that results in a possibly slimmer Jacobian matrix. In my computations, the variables are packed in a one-dimensional solution vector in such an order that the species index changes first, then the angular discretization index and then the radial discretization index. This scheme results in the Jacobian matrix with only ℓN_θ nonzero sub- and superdiagonals. As initial condition, I used the results of numerical time-integration of the reaction-diffusion system with the help of Barkley's software EZspiral. I stopped Newton iterations once the residual norm had become smaller than a given tolerance, typically 10^{-8} .

To exclude the rotation symmetry of spirals on disk, I pinned the spiral at a chosen point, prescribing a value to one of ℓ species there. Thus I obtained one variable free, and at that position in the solution vector the unknown value of the rotation frequency ω was substituted. The derivative of the left-hand side of Eq. (2) with respect to ω is given by the angular derivative of the spiral $\partial_\theta q$, which filled out a whole column in the Jacobian matrix, making it non-banded. However, this is a rank-one perturbation and can be dealt with by using the Sherman-Morrison formula [25].

I also used a primitive continuation procedure, slowly changing one of the parameters of the equations or the disk radius to obtain the spiral with desired parameter values.

b. Linear problem Once the solution of the nonlinear problem had been obtained within the desired accuracy, I built the linearization matrix and the matrix, representing the discretization of the adjoint \mathcal{L}^+ . Let me denote that finite-dimensional matrix by A . I had to compute three eigenvalues of A which were close to $0, \pm i\omega$, where ω is the rotation frequency of the computed spiral q . For that purpose, I used ARPACK library which offers an implementation of the iterative Arnoldi method for computing eigenpairs for large sparse matrices (see <http://www.caam.rice.edu/software/ARPACK/>).

ARPACK offers among others two modes of computations: for eigenvalues with largest modulus and for eigenvalues with largest real part. I experimentally found that the largest modulus mode worked faster and much more

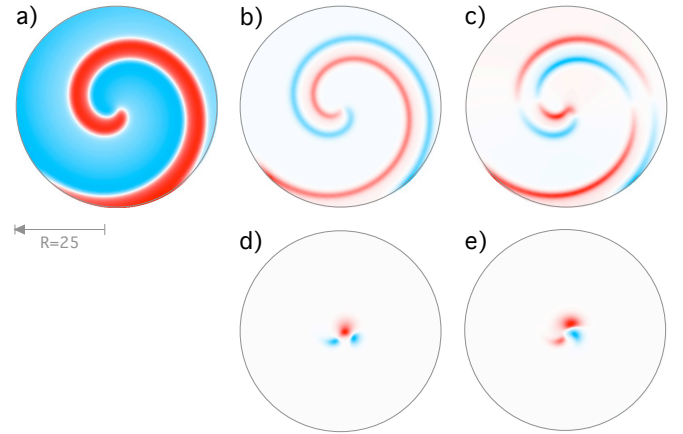


FIG. 2: a) Color-coded U -component of the spiral wave solution. b) Color-coded real part of U component of the rotational eigenfunction of \mathcal{L} . c) Color-coded real part of U component of the translational eigenfunction of \mathcal{L} . d) Color-coded real part of U component of the rotational eigenfunction of \mathcal{L}^+ (rotational response function). e) Color-coded real part of U component of the translational eigenfunction of \mathcal{L}^+ (translational response function). For all panels parameters are as in text, disk radius $R = 25$, blue values represent smaller values than the red one. For b) to e), white colour corresponds to zero level.

reliable, hence I needed to modify my matrix A and map away its critical eigenvalues at $0, \pm i\omega$ possibly far from the origin of the complex plane. As suggested in [23], I used the Cayley transformation to build another matrix B , which is related to A by

$$B = \frac{A + I\eta}{A + I\xi},$$

where I denotes the identity matrix and η and ξ are complex parameters of the transform. The eigenvalues of A which are close to $-\xi$ are mapped to eigenvalues of B with large absolute value. I hence chose $-\xi$ to be in the region of my interest, namely close to 0 and $i\omega$. The parameter η was set to $i\text{Im}\xi$.

As a convergence criterion, I used the *machine accuracy* mode of ARPACK, which resulted in convergence to the eigenpair within a few iterations. The residuals did not exceed 10^{-14} .

Allow me to stress again that on bounded disks, I expected the translational eigenvalues to be slightly off the imaginary axis. This is due to the fact that the translational invariance is broken when truncating the domain to a finite size.

IV. RESULTS

As a paradigmatic example of reaction-diffusion systems, the two-variable Fitzhugh-Nagumo system [26] was

chosen, which reads

$$\begin{aligned}\partial_t U &= \frac{1}{\varepsilon} (U - U^3/3 - V) + \Delta U, \\ \partial_t V &= \varepsilon(U - aV + b)\end{aligned}\quad (7)$$

with parameters $a = 0.5, b = 0.68$ and $\varepsilon = 0.3$.

A. Computing response functions

After a round of simulations with EZspiral, my Newton solver converged to a rigidly rotating spiral wave solution within less than 10 iterations. After that the critical modes $v_{0,\pm 1}$ of the linearization \mathcal{L} and the critical modes $w_{0,\pm 1}$ to the adjoint \mathcal{L}^+ were computed.

I first checked the biorthogonality of v_i and w_i , computing the scalar products $\langle w_i, v_j \rangle$. The difference in the magnitude of the scalar product for cases $i = j$ and $i \neq j$ was of the order 10^8 , which can be considered as a good orthogonality.

The graphical representation of the solution of the non-linear problem and examples of eigenfunctions of linearization \mathcal{L} and adjoint \mathcal{L}^+ can be found in Fig. 2. As expected, the rotation mode of \mathcal{L} is nothing else but the angular derivative of the spiral and the translational mode is just slightly rotated y derivative. Both modes are not localized as the spiral is not localized itself. In contrast to that, the response functions, both translational and rotational one, are strongly localized near the core region of the spiral. The behaviour and the localization properties of the imaginary part of U and those of V component of the Fitzhugh-Nagumo kinetics is qualitatively the same as in the presented plots for $\text{Re} U$.

Fig. 3 summarizes the results on the convergence of the method. Due to the pseudospectral discretization in angle θ , the convergence with respect to the number of angular grid points is exponential. Due to the three-point scheme for the radial derivative, the convergence in Δr is quadratic. Fig. 3 also shows that the translational eigenvalues approach the imaginary axis at an exponential rate while increasing radius of the disc.

B. Computing drift velocity

I used the response functions of spirals in the Fitzhugh-Nagumo system in order to compute drift velocities for the perturbed problem:

$$\begin{aligned}\partial_t U &= \frac{1}{\varepsilon} (U - U^3/3 - V) + \Delta U + \epsilon h, \\ \partial_t V &= \varepsilon(U - aV + b).\end{aligned}\quad (8)$$

Here h denotes the external perturbation that makes the spiral drift, and ϵ is a small perturbation strength.

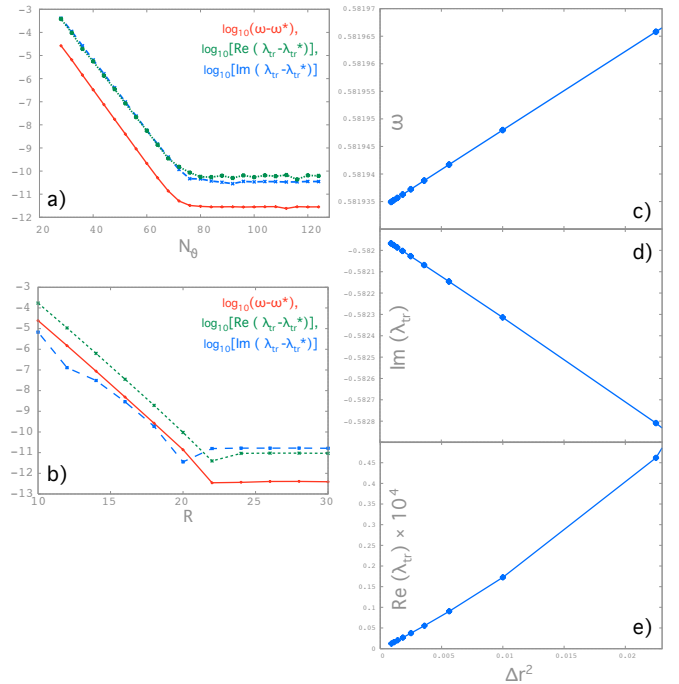


FIG. 3: a) Dependence of spiral frequency ω , real and imaginary part of translational eigenvalue on number of angular discretization points N_θ . Starred values are for $N_\theta = 128$. Other parameters as in text, $\Delta r = 0.2, R = 16$. b) Dependence of spiral frequency ω , real and imaginary part of translational eigenvalue on radius of disk R . Starred values are for $R = 32$. Other parameters as in text, $\Delta r = 0.2, N_\theta = 96$. c) to e) Dependence of spiral frequency ω , real and imaginary part of translational eigenvalue on radial discretization step Δr . Other parameters as in text, $R = 16, N_\theta = 96$.

1. Resonant drift

Here I set perturbation h to be a periodic continuation of a step function which assumes value -1 during the first half-period and 1 during the second half-period. The period of h coincides with the computed period of rotation of the spiral wave. Eq. (6) suggest that such perturbation do not influence the rotation frequency of the spiral, since it has a zero mean over the period. For simulation of spiral wave I again used Barkley's software EZspiral.

The comparison of the prediction by response functions for the magnitude of the drift and the value from direct numerical simulations is plotted in Fig. 4, panel (a). There is a nice correspondence between the prediction by response function and the results of simulation in a quite wide range of perturbation strength ϵ . At the maximal value of ϵ that I used, the drift velocity of spiral was that high that the spatial translation of the spiral between two successive rotations was comparable to the radius of the unperturbed tip trajectory.

2. Drift in inhomogeneities

Here I chose for the perturbation $h(x, y) = x - x_0$, where x is the current cartesian coordinate on the plane and x_0 is a reference point. In the rotating coordinate frame (r, θ_{rot}) associated with the spiral this perturbation becomes time-periodic $h(r, \theta_{\text{rot}}) = r \cos(\omega t + \theta_{\text{rot}})$, where $\theta_{\text{rot}} = \theta - \omega t$. Thus the spiral experience a time-periodic resonant perturbation in this case, too.

While drifting in an inhomogeneity, the spiral possible moves to regions with different value of h and its rotation frequency and spatial profile may change. This implies that in an inhomogeneous medium, the drift velocity and drift direction of the spiral is location-dependent. Since it would be quite involving to compute spiral and its response functions for several positions on the plane, I decided to choose a very mild value of the inhomogeneity gradient and try to compare two different experimental protocols for direct simulations: In the first one, I just kept the value x_0 constant close to the initial position of the spiral and in the second one I shifted x_0 together with the drift of the spiral wave tip. Results of numerical simulations according to both protocols are displayed in Fig. 4 (b). Strangely enough, but it seems that shifting the reference point x_0 together with the spiral tip doesn't produce any improvements over the static inhomogeneity.

V. CONCLUSIONS AND OUTLOOK

The results of this study suggest that response functions of rigidly rotating spiral waves in reaction-diffusion systems can be computed in a systematic manner using the freely available ARPACK library. Those response functions, being the eigenfunctions of the adjoint problem, satisfy the requirement of orthogonality to the critical eigenfunction of the linearization about spiral. They can hence be used in projections techniques for computing drift velocity under external symmetry-breaking perturbations.

Probably the main mystery for me in this story is how to bring together rigorously the theory for drifting spirals on the whole plane with the results of modeling on bounded domains. Of course, due to the localization of response functions, the spiral would not sense the presence of the boundaries in (numerical) experiments anyway, but strictly speaking, the influence of boundaries is non-zero, but rather exponentially small. Cutting the long story short, there is still no rigorous theory for spiral drift on bounded domains. Such a theory would result

in a drift velocity which should be dependent on the location of spiral relative to the domain boundaries. Even without external forcing, spirals would drift even due to the interaction with the boundaries.

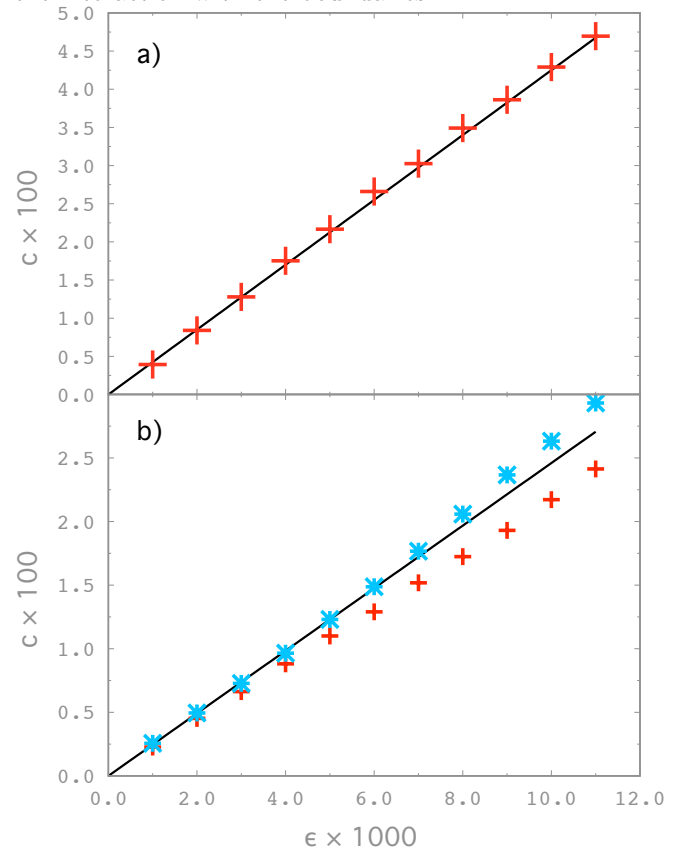


FIG. 4: Magnitude of drift velocity c as function of the perturbation amplitude ϵ . In both a) and b) straight line represent the predictions with the help of response functions. a) Crosses show results of numerical integration of spiral which was homogeneously perturbed at the frequency equal to the rotation frequency of spiral itself b) Crosses and asterisks show results of numerical integration of spiral in constant gradient. Red crosses correspond to experimental protocol 1, blueish asterisks correspond to experimental protocol 2, see text.

Acknowledgments

This study would not have been possible without Dwight Barkley, Vadim Biktashev and Irina Biktasheva. I acknowledge financial support from EPSRC and SFB 555.

-
- [1] M. Cross and P. C. Hohenberg, *Rev. Mod. Phys.* **65**, 851 (1993).
 [2] A. T. Winfree, *When Time Breaks Down: The Three-Dimensional Dynamics of Electrochemical Waves and*

- Cardiac Arrhythmias* (Princeton University Press, 1987).
 [3] R. Kapral and K. Showalter, eds., *Chemical Waves and Patterns* (Kluwer Academic Publishers, 1995).
 [4] J. Murray, *Mathematical Biology* (Springer-Verlag, New

- York, 2002).
- [5] G. Mines, *J. Physiol* **46**, 349 (1913).
 - [6] K. Agladze, V. Davydov, and A. Mikhailov, *JETP Letters* **45**, 767 (1987).
 - [7] V. Davydov, V. Zykov, A. Mikhailov, and P. Brazhnik, *Izv. Vuzov - Radiofizika* **31**, 574 (1988).
 - [8] A. S. Mikhailov, V. A. Davydov, and V. S. Zykov, *Physica D* **70**, 1 (1994).
 - [9] A. Pertsov and E. Ermakova, *Biofizika* **33**, 338 (1988).
 - [10] V. Biktashev and A. Holden, *Chaos, Solitons and Fractals* **5**, 575 (1995).
 - [11] B. Sandstede and A. Scheel, *Stability and instability of spiral waves, preprint* (2007).
 - [12] B. Fiedler, B. Sandstede, A. Scheel, and C. Wulff, *Documenta Mathematica* **1**, 479 (1996).
 - [13] B. Sandstede, A. Scheel, and C. Wulff, *J. Diff. Eq.* **141**, 122 (1997).
 - [14] B. Sandstede, A. Scheel, and C. Wulff, *IMA Volumes in Mathematics and its Applications* **115**, 249 (1999).
 - [15] B. Sandstede, A. Scheel, and C. Wulff, *J. Nonlin. Sci.* **9**, 439 (1999).
 - [16] I. Biktasheva, Y. Elkin, and V. Biktashev, *Phys. Rev. E* **57**, 2656 (1998).
 - [17] I. Biktasheva, Y. Elkin, and V. Biktashev, *J. Biol. Phys.* **25**, 115 (1999).
 - [18] I. Biktasheva, *Phys. Rev. E* **62**, 8800 (2000).
 - [19] I. Biktasheva and V. Biktashev, *J. Nonlin. Math. Phys.* **8 Supl**, 28 (2001).
 - [20] I. Biktasheva and V. Biktashev, *Phys. Rev. E* **67**, 026221 (2003).
 - [21] I. Biktasheva, V. Biktashev, and A. Holden, *Int. J. Bifurcation & Chaos* **16**, 1547 (2006).
 - [22] D. Barkley, *Phys. Rev. Lett.* **68**, 2090 (1992).
 - [23] P. Wheeler and D. Barkley, *SIADS* **5**, 157 (2006).
 - [24] B. Sandstede and A. Scheel, *Phys. Rev. E* **62(6)**, 7708 (2000).
 - [25] W. H. Press, S. A. Teukolsky, W. T. Vetterling, and B. P. Flannery, *Numerical Recipes in C* (Cambridge University Press, 1988).
 - [26] J. Nagumo, S. Arimoto, and S. Yoshizawa, *Proc. IRE* **50**, 2061 (1964).
 - [27] For a linear space with the scalar product $\langle \cdot, \cdot \rangle$, the adjoint to the given operator \mathcal{A} is such operator \mathcal{A}^+ that for any elements of the space a, b the following holds:

$$\langle a, \mathcal{A}b \rangle = \langle \mathcal{A}^+a, b \rangle.$$